Forward kinematic modelling of a regional transect in the Northern Emirates, using geological and apatite fission track age constraints on paleo-burial history

Tarapoanca, M.; Andriessen, P.A.M.; Broto, K.; Chérel, K.; Ellouz-Zimmerman, N.; Faure, J.L.; Jardin, A.; Naville, C.; Roure, F.

published in
Arabian Journal of Geosciences
2010

DOI (link to publisher)
10.1007/s12517-010-0213-3

document version
Publisher's PDF, also known as Version of record

Arab J Geosci (2010) 3:395–411
DOI 10.1007/s12517-010-0213-3

ORIGINAL PAPER

Forward kinematic modelling of a regional transect in the Northern Emirates using geological and apatite fission track age constraints on paleo-burial history

Mihai Tarapoanca · Paul Andriessen · Karine Broto · Louis Chérel · Nadine Ellouz-Zimmermann · Jean-Luc Faure · Anne Jardin · Charles Naville · François Roure

Received: 30 March 2010 / Accepted: 3 October 2010 / Published online: 2 November 2010

Abstract This paper aims to simulate the kinematic evolution of a regional transect crossing the Northern Emirates in the northernmost part of the Semail Ophiolite and the Dibba zone, just south of the Musandam Platform exposures. The studied section comprises, from top to bottom and from inner to outer zones, (1) the erosional remnants of the Semail Ophiolite, mainly made up of serpentinized ultramafics in the west and gabbros in the east, (2) high-grade metamorphic rocks which are currently exposed in the core of a nappe anticline near Masafi, (3) far-travelled Hawasina basinal units and Sumeini paleo-slope units of the Dibba Zone, (4) parautochthonous platform carbonates, which are currently well exposed in the Musandam area, and (5) a flexural basin filled with uppermost Cretaceous to Neogene sediments. Two main compressional episodes are generally identified, resulting first in the obduction of the Semail Ophiolite and then in the stacking of underlying platform carbonate units of the former Arabian passive margin, thus accounting for the present architecture of this transect: (1) first, deformation at the plate boundary initiated in the Late Cretaceous, resulting in the obduction of the Semail Ophiolite and the progressive accretion of the Hawasina and Sumeini tectonic wedge on top of the Arabian foreland, leading to a progressive bending of its lithosphere and development of a wide flexural basin; (2) compression resumed during the Neogene, leading to the tectonic stacking of the parautochthonous platform duplexes of Musandam and Margham trends, the development of out-of-sequence thrusts and triangle zones, refolding of the sole thrust of the former Late Cretaceous accretionary wedge and coeval normal (?) high-angle faulting along the contact between the Musandam and Dibba zones. However, seismic profiles and paleo-thermometers also help in identifying another erosional event at the boundary between the Paleogene Pabdeh and the Neogene Fars series. Evidenced by the local erosional truncation of the Pabdeh series in the vicinity of the frontal triangle zone (i.e. the inner part of the former Late Cretaceous foredeep), this Paleogene uplift/unroofing episode is tentatively interpreted here as an evidence for a continuum of compressional deformation lasting from the Late Cretaceous to the Middle Miocene although one may alternatively speculate that it was related to the detachment of the subducted slab. Although carbonate facies are usually not suitable for apatite fission track (AFT) studies, we were able to extract detrital apatites from quartz-bearing Triassic dolomites in the Musandam area. However, the yield and the quality were both poor and too few fission track lengths could be measured, making it difficult to interpret the meaning of the FT ages. The FT dates obtained in this study are therefore compared with those existing in

M. Tarapoanca · K. Broto · L. Chérel · N. Ellouz-Zimmermann · J.-L. Faure · A. Jardin · C. Naville · F. Roure
IFP Energies nouvelles,
1-4 Avenue de Bois-Préau,
92 Rueil-Malmaison, France

P. Andriessen · F. Roure
Faculty of Earth and Life Sciences, VU-University,
de Boelelaan 1085,
1081 HV Amsterdam, The Netherlands

Present Address:
M. Tarapoanca (✉)
Danubian Energy Consulting,
42-44 Vasile Lascar, 5th Floor, 11th Suite,
Bucharest 020492, Romania
e-mail: mtarapoanca@danubianenergy.com

the literature. Fortunately enough, for each sample, at least ten apatite crystals could be used for fission track dating, except for site 6 with only five datable apatite grains. The obtained apatite fission track dates between 28 and 13 Ma, much younger than the Triassic age of the series, are taken to represent reset fission track ages, implying erosion of an up-to-3-km-thick pile of Jurassic–Cretaceous carbonates and Hawasina allochthon during the Neogene. Apatite fission track dates from the ~95 M-old plagiogranites of the Semail complex (Searle and Cox, *Geol Mag* 139 (3):241–255, 2002) obtained in this study and compared with those recently published provide evidences for more than one cooling event. An early unroofing of the ophiolite during the Late Cretaceous is revealed in fission track dates of 72–76 Ma at the top of the ophiolite in the east, which are coeval and also consistent with the occurrence of paleo-soils, rudists and paleo-reefs on top of serpentinized ultramafics in the west. High-pressure rocks at As Sifah in the southeast near Muscat revealed apatite fission track data ranging from ~46 to 63 Ma (Gray et al. 2006). The leucocratic part of the ophiolite (sample UAE 180) yielded comparable young apatite (40.6±3.9 Ma) and zircon (46.6± 4.3 Ma) FT dates. A Cenozoic (~20–21 Ma) exhumation has been determined for the Bani Hamid metamorphic sole in northern Oman, applying low temperature geochronology and combining apatite FT and apatite (U–Th)/He analyses (Gray et al. 2006). In this study, young apatite fission track dates of 20 Ma have also been found but at the base of the ophiolite near Masafi, in the core of the nappe anticline, thus indicating a Neogene age for the refolding of the allochthon and stacking of underlying parautochthonous platform carbonate units. During the subsequent 2D forward Thrustpack kinematic modelling of the regional transect, these AFT data-set has been used, together with available subsurface information, to reconstruct the past architecture of the structural sections through time, accounting for incremental deformation along the various decollement levels, synorogenic sedimentation and erosion, as well as for successive bending and unbending episodes of the Arabian lithosphere.

Keywords Kinematic modeling · Oman Mountains · Fission tracks · Tectonics

Introduction

The Oman Range and northern Emirates foothills constitute a rather frontier area for petroleum exploration. However, a better understanding of thermal and subsidence versus uplift evolution of this foreland fold-and-thrust belt was required to address properly its petroleum appraisal and evaluate the exploration risks related to specific parameters such as the occurrence of potential traps, the timing of structural closures, source rock maturation and hydrocarbon migration and charge, as well as the distribution of potential source rocks, reservoirs and seals.

In this scope, four deep seismic profiles, i.e. two dip and two strike profiles, were recently recorded by Western-Geco on behalf of the Ministry of Energy of the UAE, extending onshore of the Northern Emirates, mainly in the foothills part of the Oman Range (Styles et al. 2006) (Fig. 1). Because only a portion of the autochthonous foredeep basin develops onshore (western portion of D1 and D4 lines), industry lines provided by Sharjah and Dubai Ministries from the Arabian Gulf offshore have also been integrated in this study in order to get a better control on the evolution of the Late Cretaceous flexural basin. Industry lines provided by the Ministry of Fujairah were also integrated in this project in order to get some control on the architecture of the hinterland, in the Fujairah offshore.

These deep seismic profiles were depth-migrated and combined with industry lines, wells data and outcrop studies, the two dip lines D1 and D4 being then used to constrain structural sections along two regional transects crossing the Oman Range and their adjacent foreland from the Oman Gulf in the east up to the Arabian Gulf in the west. Upon restoring the transects to pre-obduction times, forward coupled kinematic and thermal modelling using the Thrustpack software (last detailed description of Thrustpack in Sassi et al. 2007), was subsequently performed along them in order to propose realistic scenarios for the burial of Mesozoic source rocks and reservoirs and to better understand the evolution of the plumbing system (migration pathways for the hydrocarbons between mature kitchens and potential traps; Roure et al. 2006).

This paper focuses on the northernmost profile (D4) and aims at discussing its present architecture and presenting the results of its Thrustpack forward kinematic modelling as well as apatite fission track analyses (AFT) performed at VU-Amsterdam that were done according to standard procedures and techniques described in, for example, the PhD thesis of Necea (2010). The FT zircon age determination was done according to standard techniques using EDM and revealing fission tracks in zircon using chemical etching of KOH–NaOH eutectic melt at 220°C for 36 h. Fluid flow modelling performed with Ceres 2D along the same transect is discussed in a companion paper (Callot et al. 2010).

Regional geological background and overall architecture of the cross-section

The northern Emirates comprise various tectono-stratigraphic domains (Figs. 1 and 2):

– (1) The Paleozoic and Mesozoic series of the former passive Arabian margin, which comprise thick platform

reservoir carbonates ranging from Permian (Khuff) to Middle Cretaceous (Thammama) and intervening source rock and local evaporites (Robertson and Searle 1990).

– (2) A Late Cretaceous–Cenozoic foreland basin made up of Late Cretaceous (Aruma Group), Paleogene (Pabdeh) and Neogene (Fars) clastics, separated by an evaporitic interval (Massive and Cyclic Salt formations) which covers the western onshore province (lowlands) and adjacent offshore of the Arabian Gulf (Patton and O'Connor 1986; 1988; Boote et al. 1990; Warburton et al. 1990; Béchennec et al. 1995).
– (3) A Late Cretaceous–Cenozoic fold-and-thrust belt, which accounts for the current elevated topography of the Oman Range (Glennie et al. 1973, 1974; Graham 1980a; Ricateau and Riché 1980; Lippard et al. 1982; Searle et al. 1983; Searle 1985, 1988a, b; Gass and Shelton 1986; Hanna 1986, 1990; Dunne et al. 1990; Le Métour et al. 1990; Robertson et al. 1990; Warrak 1996; Breton et al. 2004; Glennie 2005). This belt extends over the eastern portion of the Emirates, with wide exposures of peridotite in the south (Semail ophiolite; Gealey 1977; Coleman 1981; Goodenough et al. 2010), dominantly Permian to Cretaceous platform carbonate outcrops in the north (Musandam Peninsula, partly in Oman) and an intervening domain, the Dibba Zone, where Mesozoic Sumeini slope and Hawasina basinal units are still locally preserved (Graham 1980b; Watts 1985, 1990; Watts and Garrison 1986; Bernoulli and Weissert 1987; Béchennec et al. 1988, 1990; Watts and Blome 1990; Eilrich and Grotsch 2003). Along the southeastern border of the Musandam carbonate units, thick Upper Cretaceous (Cenomanian to Campanian?) carbonate breccias of the

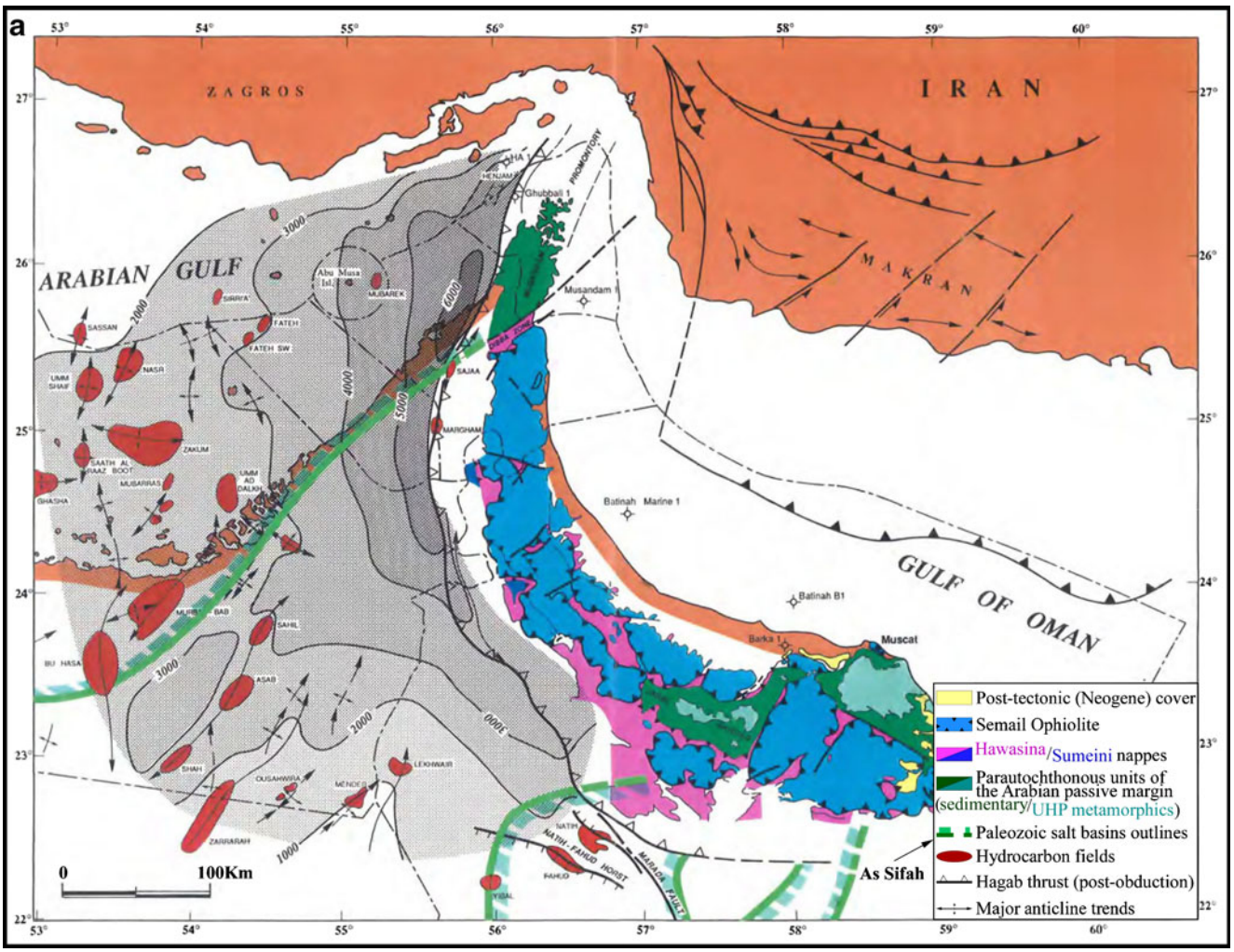

Fig. 1 **a** Structural map of the Emirates and Oman Range (after Bois et al. 1990). Isobaths (metres) are an estimate of the depth to the foreland base. **b** Structural map of the Northern Emirates outlining the location of the D1 and D4 seismic traverses as well as the location of the AFT samples. Notice the regional unconformity at the base of the Cretaceous breccia, which rests unconformably on top of underlying Lower Cretaceous, Jurassic, Triassic and even Permian series

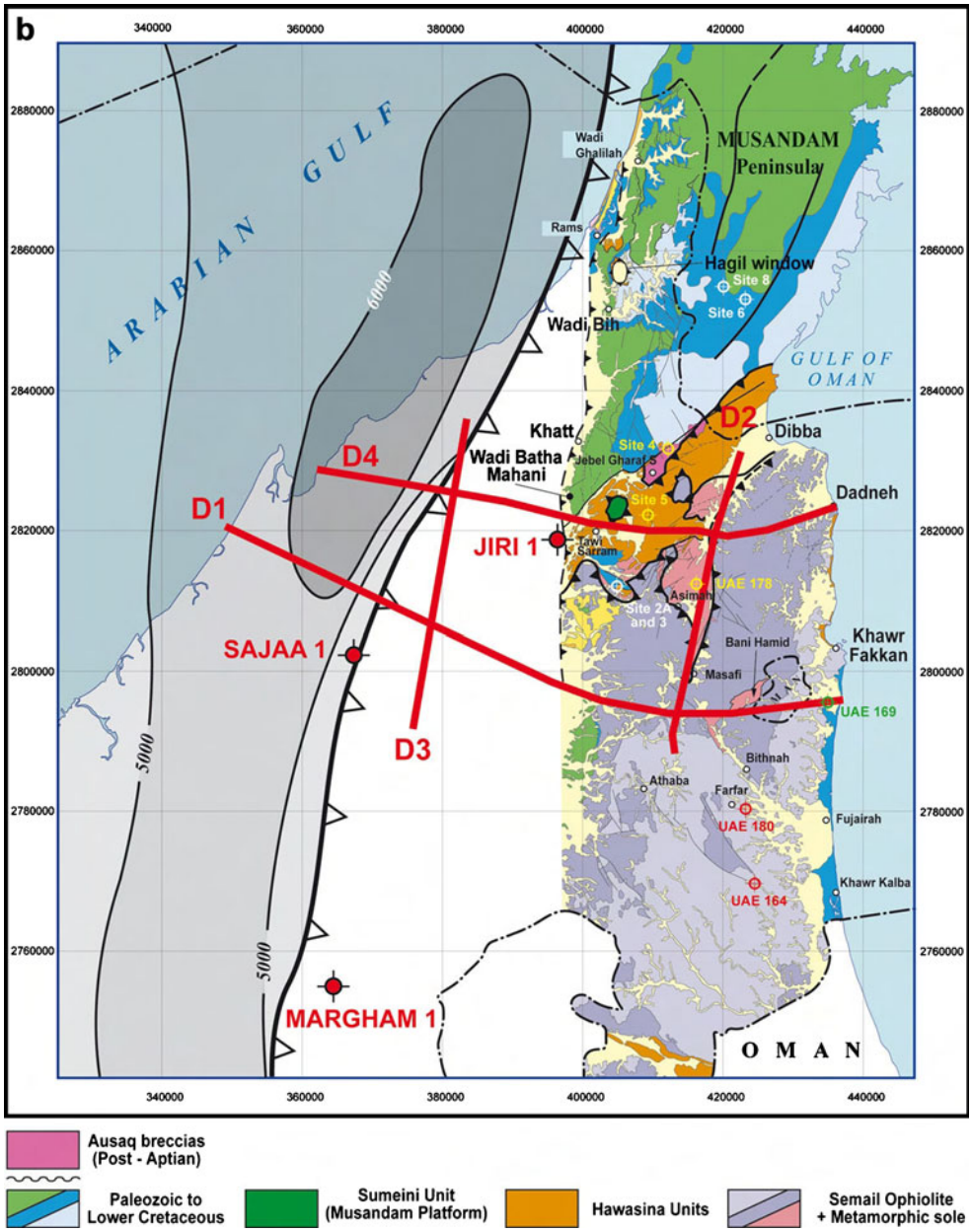

Fig. 1 (continued)

Ausaq Formation rest unconformably on top of older Jurassic, Triassic and even Permian series, in the footwall of the Sumeini–Hawasina allochthon (Ellison et al. 2006; Phillips et al. 2006), indicating that uplift (of at least part of the foreland) took place before the obduction of the Semail ophiolite. Whether this unconformity is genetically related to an early inversion of the Arabian plate, flexural bulging with/without a eustatic sea level drop or others remains unknown.

– (4) A Late Cretaceous–Cenozoic hinterland basin (Coffield 1990), dominantly filled with the erosional products of the Oman Range, which extends in the Fujairah offshore and laterally connects with the oceanic domains of the Gulf of Oman and Indian Ocean.

The overall structural style of the Oman foothills is well documented along profile D4, with a major decoupling occurring between the far-travelled basinal Hawasina–Sumeini allochthon and underlying platform carbonate units (Figs. 3 and 4). A major regional backthrust (frontal triangle) develops within the dominantly ductile Late Cretaceous–Cenozoic clastics of the flexural series in the foredeep basin, which becomes progressively tilted and uplifted by the underlying tectonic wedge made up of brittle carbonate units (Figs. 3, 4 and 5).

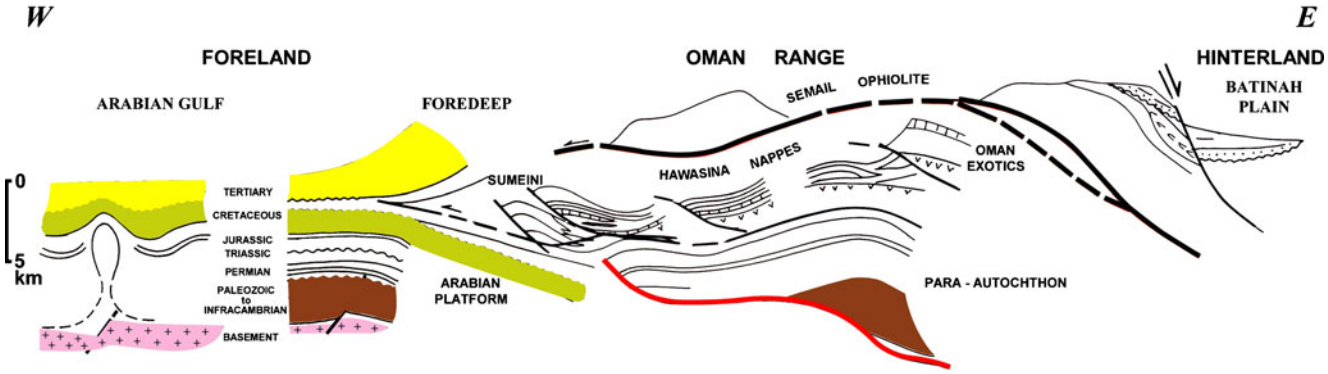

Fig. 2 Synthetic diagram outlining the architecture of the main tectono-stratigraphic units of the Northern Emirates (after Bois et al. 1990)

Cenozoic up-thrusts made up of platform carbonates are well imaged in the central part of profile D1 near Sajaa and on profile D4 just to the east of intersection with D3, where they account for the refolding of the former sole thrust of the Sumeini–Hawasina allochthon. In addition, deep carbonate duplexes are also imaged beneath the Musandam unit in the central portion of D4, as well as on orthogonal industry profiles, implying a local tectonic duplication of the Arabian platform (Figs. 3 and 4). These duplexes can still be followed toward the south on line D1 and industry profiles, with a progressive decrease in the amount of horizontal offset. This trend is reflected in topography by the high elevation, up to 1,500 m above sea level, of the currently exhumed Musandam unit in the north, whereas

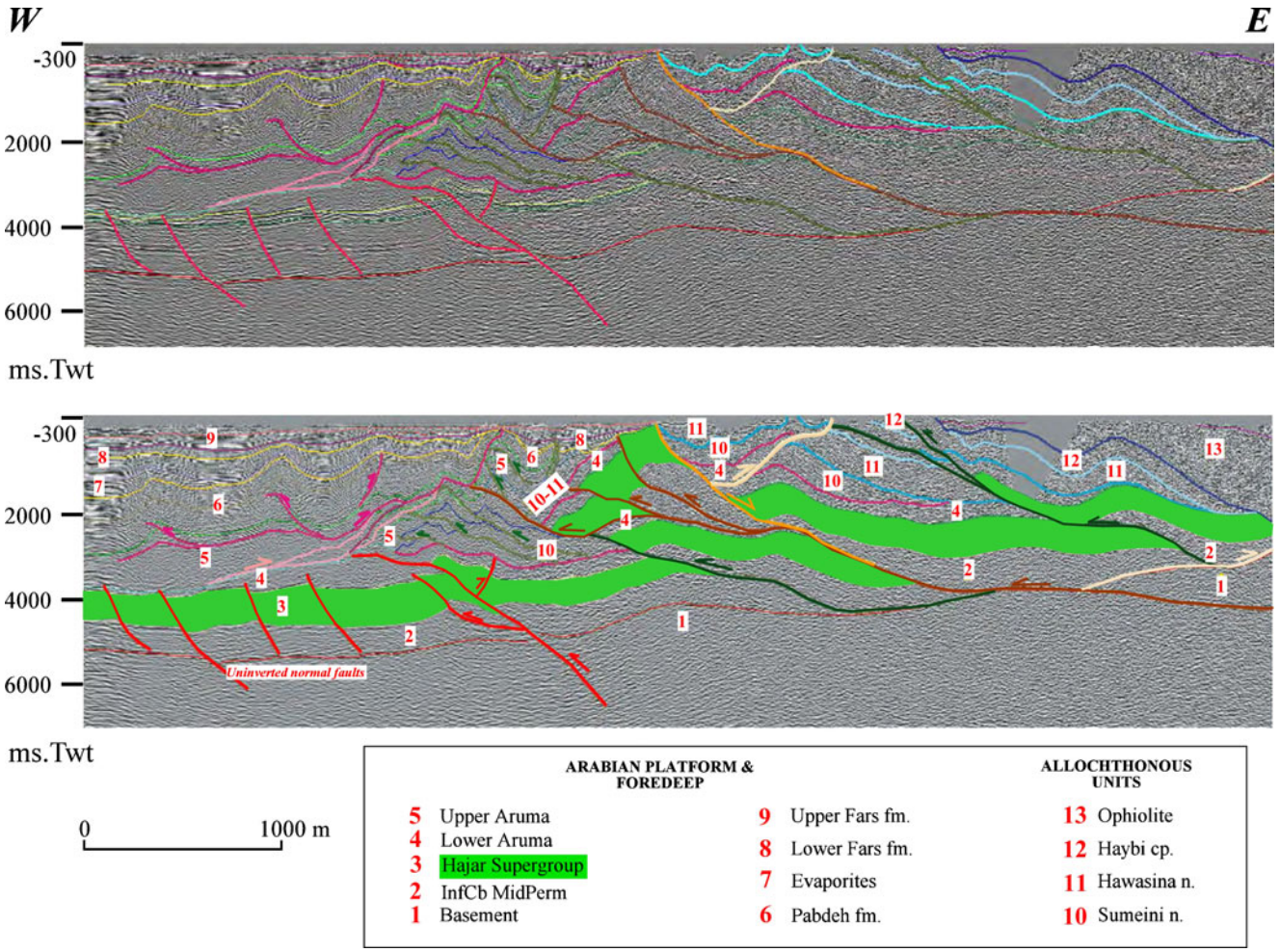

Fig. 3 Stratigraphic and structural interpretation of profile D4 (time section)

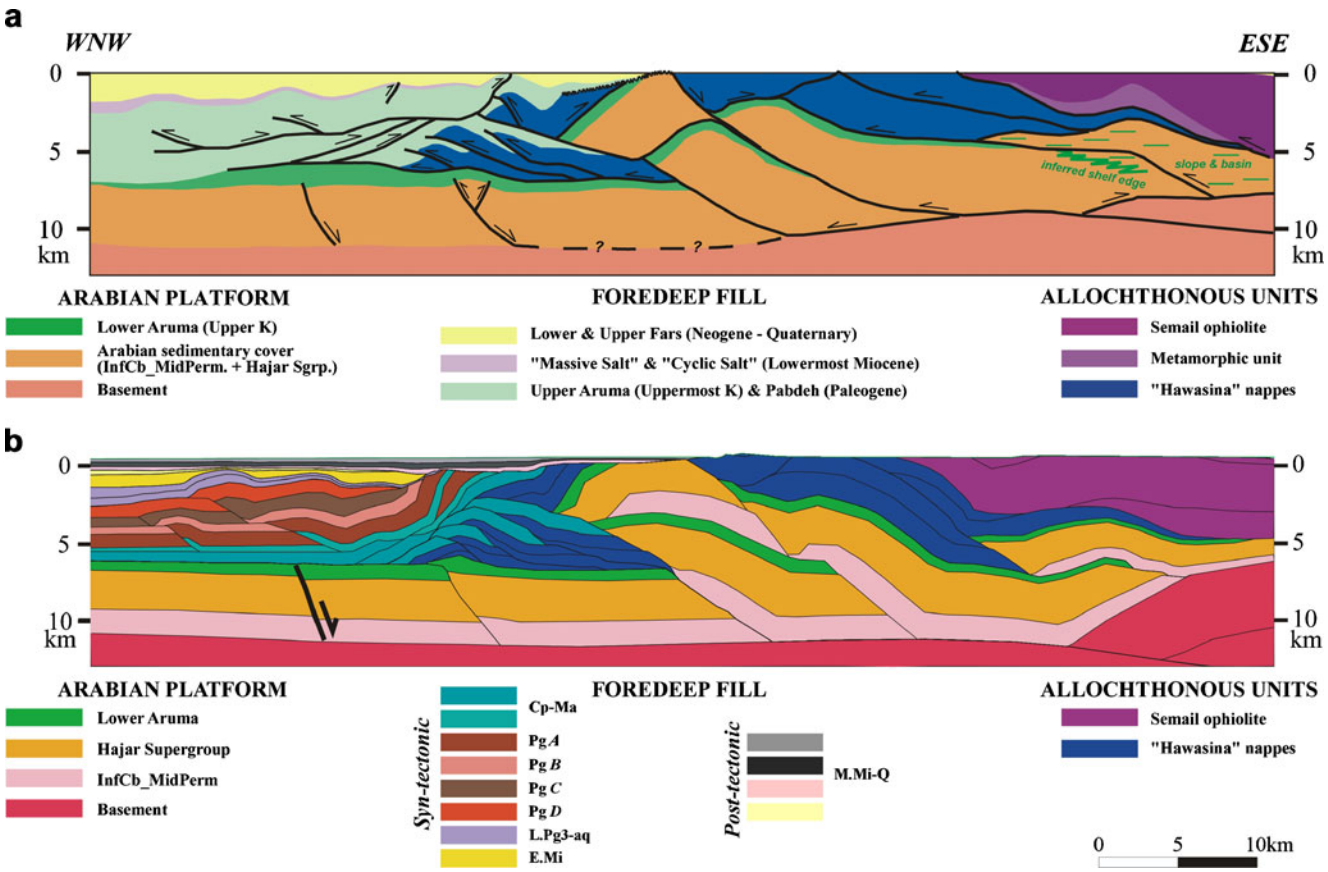

Fig. 4 **a** Present-day architecture of the regional transect D4, as derived from the interpretation of the depth-migrated seismic profile. **b** Result section of the Thrustpack model

similar platform carbonate units still remain deeply buried farther to the south.

The Hawasina–Sumeini allochthon as well as its post-obduction sedimentary cover is intensively deformed by west-verging out-of-sequence thrust faults. Actually, the detailed structural architecture changes from north to south, i.e. from D4 to D1: In the north (profile D4), a tectonic outlier made up of Hawasina–Sumeini material is carried passively above a deeper decollement, in front of the still advancing Musandam unit, both units being truncated by an Early Miocene unconformity, whereas in the south (profile D1) the lateral equivalent of Musandam parautochthonous unit is overlain by an older out-of-sequence contact involving the Hawasina–Sumeini allochthon and unconformable Upper Aruma and possibly even Paleogene cover.

Ultimately, a regional east-dipping high-angle normal fault is interpreted in the central part of profiles D1 and D4, accounting for a steep vertical offset of Mesozoic carbonates along the southeastern border of the Musandam outcrops (Figs. 3 and 4). This fault becomes listric at depth, where it roots down to the basal decollement. However, as we did not observe directly the fault scarp at the surface, we cannot preclude that this fault had also an out-of-the plane transport component. It is likely that this fault also acts as a tear fault or lateral ramp, thus accounting for a dominantly right-lateral strike–slip motion at the boundary between the Hawasina–Sumeini far-travelled basinal allochthon of the Dibba Zone and the adjacent, only moderately transported Musandam platform carbonate units.

New constraints on the tectonic deformations

The seismic profiles D1 and D4 provide a continuous and clear image of synorogenic sediments which are still preserved west of the Musandam carbonates and Semail Ophiolite. The internal architecture of seismic reflections outlines a number of tectonic imbrications, unconformities and growth strata that have been calibrated at a regional scale using several exploration wells, thus providing an accurate tectonic insight.

New apatite fission track dating has been dedicated to the Musandam carbonates and plagiogranites (with one zircon FT analysis) exposed within the Semail Ophiolite, thus providing additional constraints on the timing of tectonic uplift and erosional unroofing of the foothills.

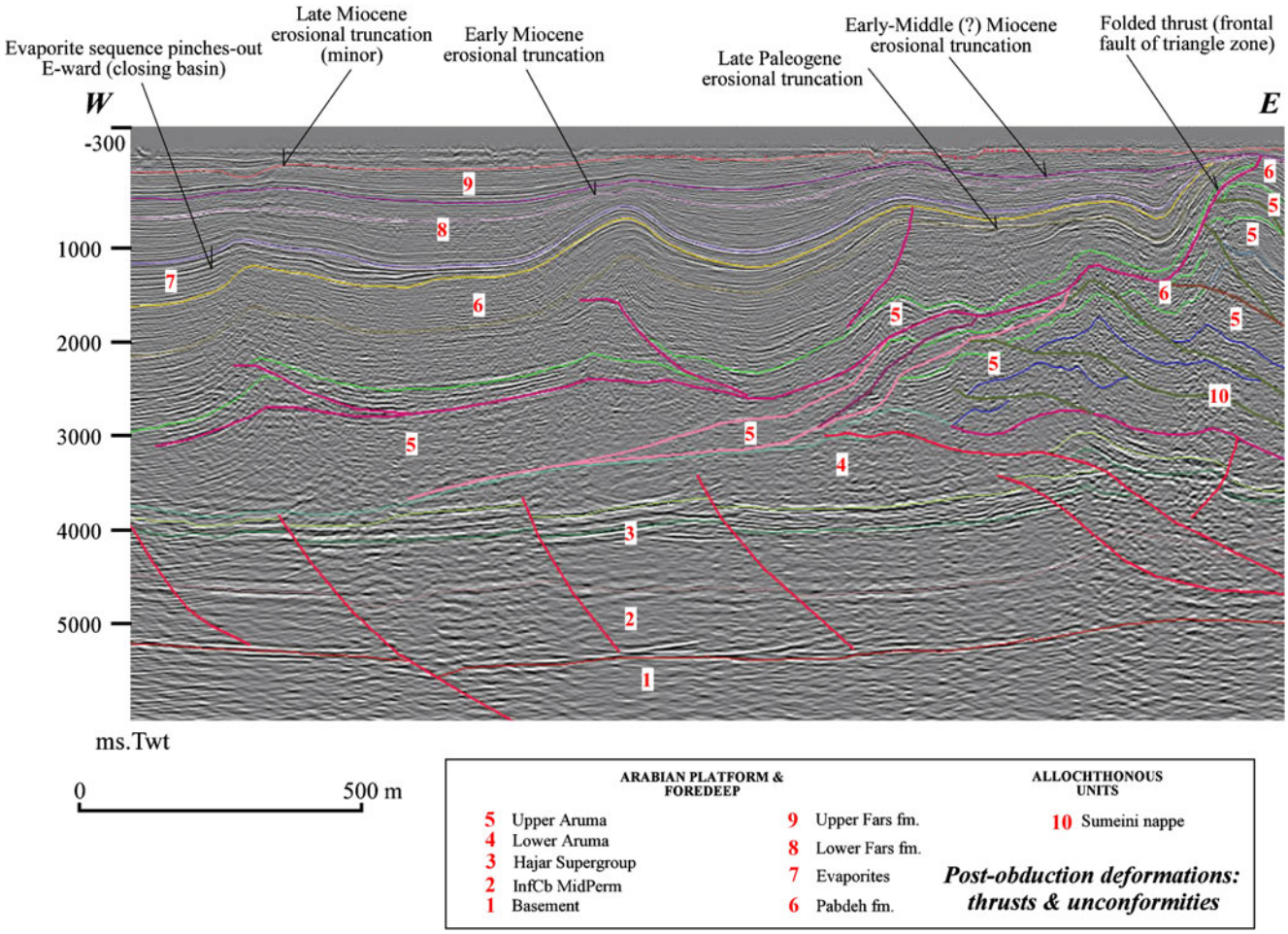

Fig. 5 Extract from seismic profile D4 (time section) outlining the main synorogenic series as well as the architecture of the frontal triangle. Notice the present unbending altitude of the Arabian platform (*1*, *2* and *3*), the eastward thickening Upper Cretaceous flexural sequence (Aruma Group; *4* and *5*), the strong erosional truncation of the Paleogene series (Pabdeh Formation; *6*) below the basal unconformity of the Neogene series (*7*) in the eastern part of the section, the progressive eastward onlaps of the Neogene evaporites (*7*) and the growth strata imaged in the Lower and Upper Fars series (*8* and *9*), which are indicative of the Neogene deformation of the frontal triangle

Synflexural and synkinematic sedimentation and timing of the deformation

Seismic stratigraphy on profile D4 (Figs. 3 and 5) and wells calibration (e.g. Jiri well) provide key information on the overall tectonic history of the Northern Emirates. The numbers in the text below refer to stratigraphic codes used in Figs. 3 and 5:

- In all the foreland part of the sections, the top of platform carbonates of the Hajar Supergroup (Lower Cretaceous, labelled as number 3) is well imaged, accounting for highly reflective horizons dipping slightly to the east, thus outlining the foreland regional flexure.
- During Aruma time (Upper Cretaceous, horizons labelled 4 and 5), a flexural sequence develops in the foreland, accounting for a progressive eastward thickening of both the Lower and the Upper Aruma (4 and 5) in the autochthon. In the foothills domain, in contrast, Aruma stage records the initial thrust emplacement of the Hawasina–Sumeini allochthon (labelled 10 and 11), which is partly overriding the Lower Aruma sequence (Santonian, labelled 4) but is also unconformably overlain by the Upper Aruma sequence (Campanian–Maastrichtian, labelled 5) or rests locally on top of Semail ophiolite farther to the south along profile D1.
- During Pabdeh time (Paleocene to Oligocene, horizons labelled 6), two different interpretations are still debated:

  (1) In the first interpretation, internal imbrications could predate the overlying Neogene unconformity, thus accounting for the continuous shortening and stacking of basinal units and the early development of a

frontal triangle zone, which would induce the progressive westward tilting and westward thickening of Pabdeh series (foreland-dipping monocline) above an already active regional backthrust. This hypothesis was favoured in the kinematic reconstruction of Fig. 6.

(2) Alternatively, the erosional summital truncation of the Pabdeh series in the innermost part of the Ras-Al-Kaimah foredeep could be interpreted as the result of a more regional unbending episode, resulting from a hypothetical slab detachment. In this case, slab detachment is only speculatively introduced because strong evidences do not exist for the moment. Such regional unconformity is indeed well expressed in the autochthonous foredeep of the Zagros Mountains in offshore Iran, away from the deformation front of the Oman Range (Jahani et al. 2009), whereas additional evidence of post-Cretaceous rebound is indicated in the Central Oman foreland by the west-dipping attitude of the autochthonous Arabian platform and basement beneath the Hawasina allochthon (Boote et al. 1990). In this hypothesis, the onset of tectonic imbrication observed within the Pabdeh series would rather post-date the Pabdeh deposition, being instead coeval with the Neogene deposition of the overlying Fars series.

In both hypotheses, active wedging of the Paleogene poorly compacted sediments was induced by the westward propagation of brittle units made up of Hawasina–Sumeini material (this process is best described as "crocodile tectonics", the opening of the frontal triangle, so-called mouth of the crocodile, being related to the westward motion of the Hawasina–Sumeini wedge).

- Tectonic contraction in the frontal triangle is indeed better documented during the sedimentation of the evaporites and Asmari series (Late Oligocene–Earliest Miocene, labelled 7), although a discrete number of growth anticlines subsequently developed in the foreland above the frontal backthrust, thus segmenting the former foreland-dipping monocline in a number of individual sub-basins.
- These growth anticlines still increased their structural culmination during Lower Fars time (Early Miocene, labelled 8), synchronously with ongoing subsidence in the outer zones, whereas both deformation and subsidence became very limited during Upper Fars time (Middle–Late Miocene, labelled 9) and onwards (Plio-Quaternary). A major truncation is also imaged between Lower and Upper Fars sequences (labelled 8 and 9, respectively) in line D1 near crossing with D3 and in D4 between D3 and Musandam outcrops (Fig. 5).

Apatite fission track age determinations

Recent low temperature geochronology in Oman Mountains reveals the following results and interpretation. Apatite FT and apatite (U–Th)/He analyses in the Oman Mountains indicate a Cenozoic exhumation history with rapid cooling at 25±2 Ma from temperatures >110°C for the metamorphic sole. A more moderate post-metamorphic cooling from a shallower crustal level ~70°C between ~46 and 63 Ma for the high-pressure eclogites at As Sifah in the southeast near Muscat is revealed by apatite fission track analysis (Gray et al. 2006). U–Pb zircon ages from the plagiogranite and ^{40}Ar–^{39}Ar age determinations of hornblende from the gabbro revealed ages around 93–96 Ma, similar to ^{40}Ar–^{39}Ar ages of hornblende of the metamorphic sole between ~92 and 96 Ma and overlapping the ^{40}Ar–^{39}Ar ages between ~88 and 96 Ma of micas of the metamorphic sole (Miller et al. 1999; Searle and Cox 2002).

In this study, other lithologies were sampled. Carbonates and peridotites are usually not suitable to provide apatite crystals. Nevertheless, more than ten apatite grains (except for sample UAE 169 with only two apatite grains and sample site 6 with only five apatite grains) from various lithologies were obtained to perform FT age determinations. The poor apatite yield and quality of the grains prohibited to measure enough fission tracks lengths. The number of lengths that are measured, sometimes not more than one or two lengths and a maximum of not more than eight lengths, is too low to be considered representative. D_{par} measurements were performed in order to detect possible variations in the chemical composition of the apatites. The large variations in the measured D_{par} values in apatite grains might explain why some grains are more retentive to thermal annealing than others. The measured D_{par} values are between 2.5 and 4 μm for all samples, showing that variation in chemical composition does not play a significant role. The newly obtained age constraints are used to constrain the unroofing history of the Musandam carbonates, Dibba zone and Semail Ophiolite (Figs. 2 and 7; Tables 1 and 2):

Musandam Platform unit

Sites 6 and 8 are located in the Omani part of the Musandam platform unit and relate to quartz-bearing Triassic dolomites, whereas site 4 belongs to Upper Cretaceous (Turonian or younger according to nannofossil assemblages studied by Carla Müller) synflexural clastics which are part of the same tectonic unit and are exposed in the footwall of the Hawasina–Sumeini allochthon along the northern border of the Dibba Zone.

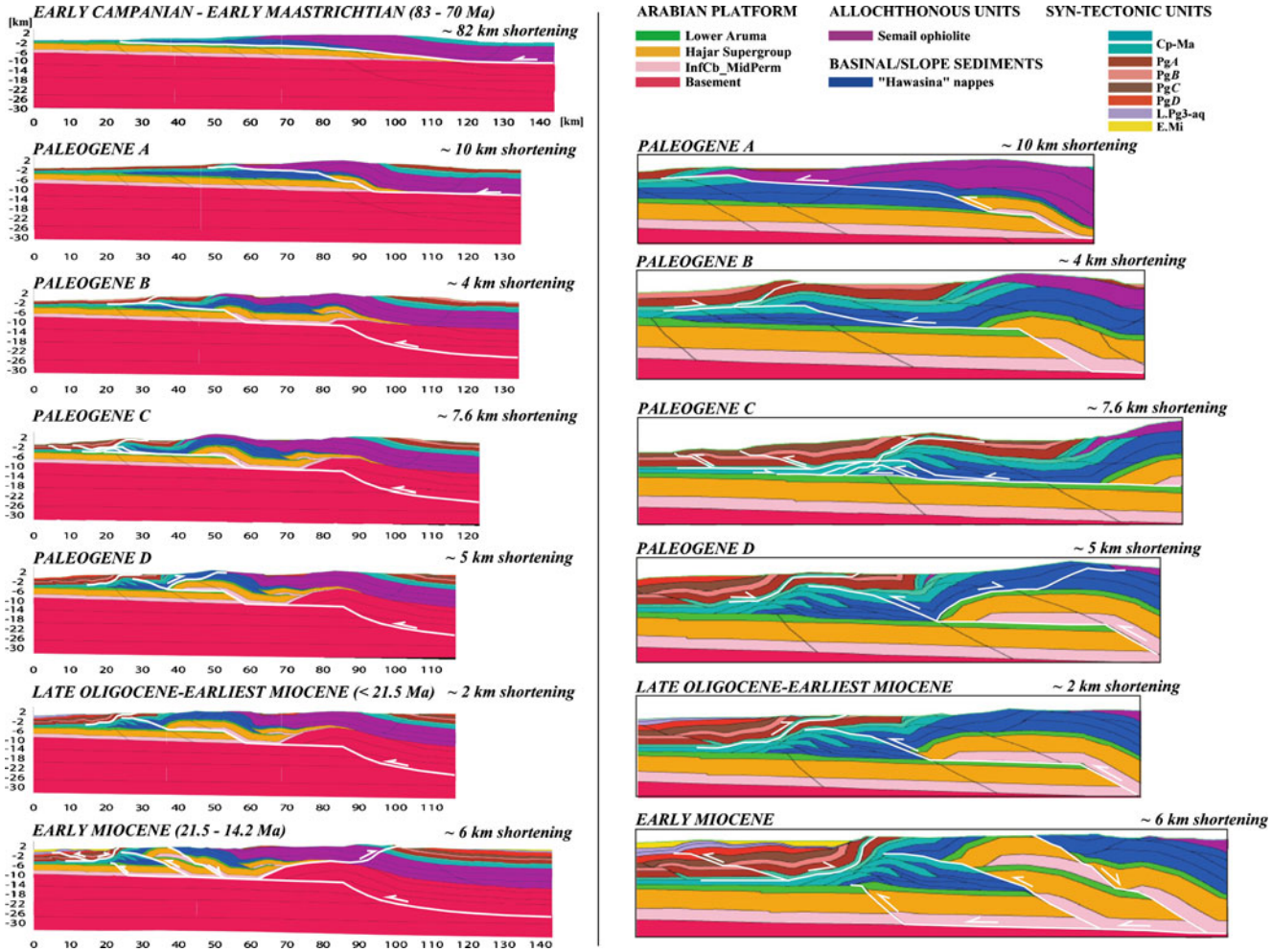

Fig. 6 Selected restoration stages of the Thrustpack forward kinematic modelling along profile D4 to be compared with the structural section of Fig. 4. The *right panel* comprises details of the modelled structural geometry. Faults active during the corresponding time span are drawn in *white*

Despite the cartographic evidence of a major erosional unroofing of the Musandam Platform before the deposition of the Upper Cretaceous breccias and overlying flexural sequence, which effectively rest locally unconformably on top of Jurassic, Triassic and even Permian series, all these samples, no matter if they are located below or above the intra-Cretaceous unconformity, display Late Oligocene or Neogene FT ages, 28.3 ± 4.7 Ma for site 4 (Upper Cretaceous clastics), 13.6 ± 3.8 Ma for site 6 (Triassic dolomite) and 15.4 ± 2.8 Ma for site 8 (Triassic dolomite). For these samples, no single apatite grain yielded a fission track apparent date older than 55 Ma, indicating that subsequent burial beneath the Hawasina–Sumeini allochthon was sufficient to (nearly) completely anneal the fission tracks and severely reset the FT apatites systems, both in the Triassic and Upper Cretaceous samples. Without information on the fission track lengths distribution, one should always be careful in interpreting the obtained fission track age data.

Sumeini and Paleozoic blocks of the Dibba Zone

Sites 2A and 3 belong to Paleozoic quartzites from the Jebel Qumar South, in the western part of the Dibba Zone, whereas site 5 relates to Upper Cretaceous (Turonian or younger according to the nannofossil assemblages studied by Carla Müller; Roure et al. 2006) synflexural clastics that rest in stratigraphic contact on top of older Sumeini slope facies of Jebel Agah, also part of the Hawasina–Sumeini allochthon infilling the Dibba Zone.

As in the Musandam unit, FT ages of the Dibba Zone display dominantly Neogene ages, averaging 27.4 ± 5.5 Ma for site 2A and 23.3 ± 2.6 Ma for site 3, both in Paleozoic quartzites, and 15.4 ± 2.8 Ma for site 5 in the Late Cretaceous synflexural sequence associated to the Sumeini slope units. Unlike in the Musandam samples, however, some grains within these samples yield older, even Cretaceous (100 Ma) apparent FT dates, suggesting that the Late Cretaceous burial of these samples was perhaps not

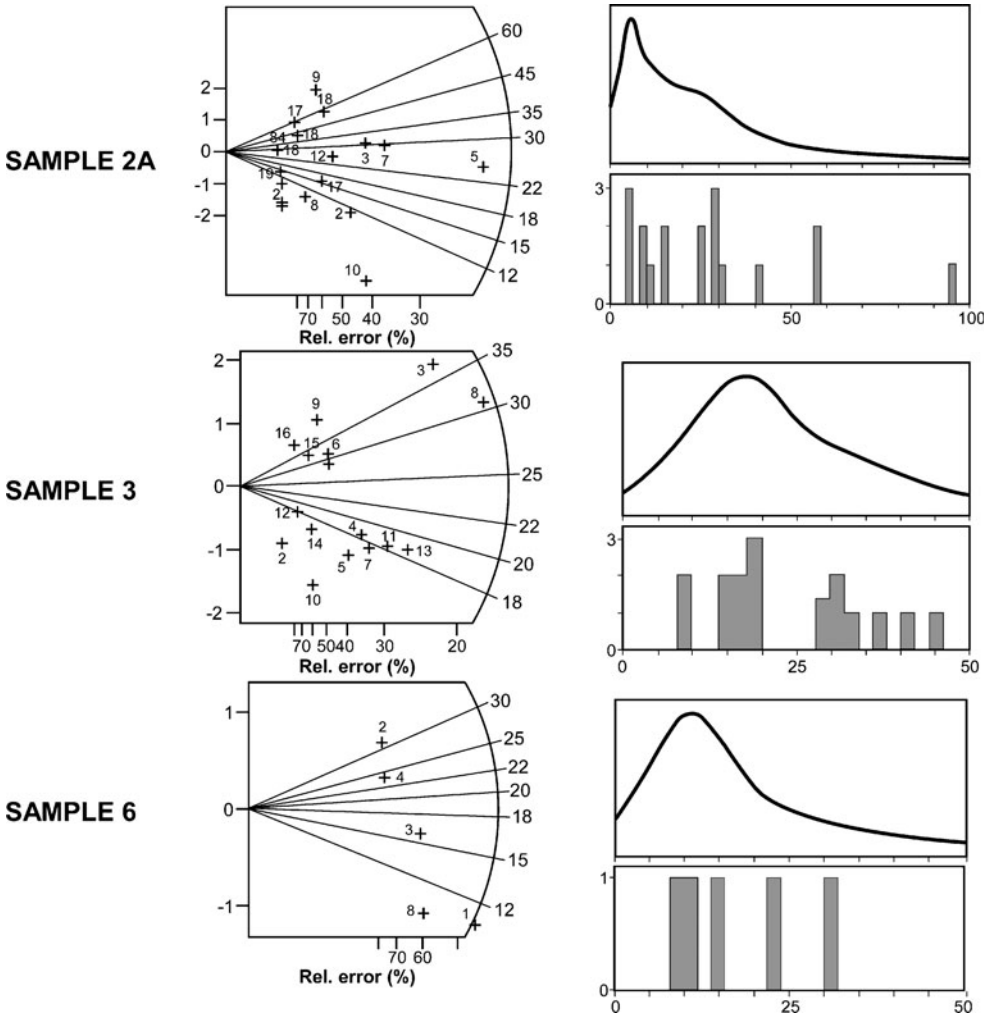

Fig. 7 Plot of AFT results of sites *2A*, *3* and *6*. Most grains have been reset during the Late Cretaceous episodes of maximum burial and record the rapid Neogene unroofing

sufficient to totally reset some of the apatite grains. Without information on the fission track lengths, interpretation is hampered. However, D_{par} measurements do not indicate a variation in the chemical composition of the apatite grains and therefore it is more likely that these samples were located at a shallower structural level than the Musandam unit, away from the erosional front of the Semail Ophiolite which constitutes the topmost unit of the tectonic pile.

Plagiogranites of the Semail Ophiolite

Surprisingly enough, a number of plagiogranitic plugs occur within the Emirati part of the Semail Ophiolite, both near the current erosional top of this unit near Fujjairah and near the sole thrust of this unit, in the core of the Masafi nappes anticline. Zircons and other heavy minerals were already extracted and separated by BGS colleagues for the purpose of radiometric dating of these plutons when we realized that apatites, if any, would be helpful also to control the timing of their tectonic uplift and erosional unroofing. U–Pb dating of zircons of the plagiogranite yielded ages of ~93–96 Ma, overlapping ^{40}Ar–^{39}Ar ages of hornblende and micas and thus pointing to rapid early cooling.

Two samples (UAE 164 and 169) from the easternmost and uppermost part of the ophiolite yield relatively old (72.6 ± 11.0 and 76.4 ± 12.8 Ma; only two grains, respectively) Cretaceous ages of unroofing, which are consistent with the occurrence of paleosoils and rudist-bearing deposits along the western side of the ophiolitic complex (Woodcock and Robertson 1982; Hamdan 1990; Nolan et al. 1986, 1990). This implies that the ophiolite was already deeply eroded during its tectonic transport, piggy-back of the Hawasina–Sumeini accretionary wedge, a long time before it reached its current structural position on top of the Arabian Platform. The relatively old apatite fission track ages show that indeed the rocks were cooled rapidly after crystallization and were emplaced close to the surface.

The sample UAE 178, located in the core of the Masafi window, very close to the base of the ophiolite, displays a Neogene age (20.3 ± 3.2 Ma), which agrees with the young age proposed for the thick-skinned tectonic accretion of the Arabian basement at the inner base of the tectonic pile,

Table 1 Apatite fission track analytical data of sedimentary samples (see the location of the samples in Fig. 1b)

Sample apatite	Rock type	Number of grains	ρ_d 10^6 tr/cm^2 (N_d)	ρ_s 10^6 tr/cm^2 (N_s)	ρ_i 10^6 tr/cm^2 ($_i$)	P (χ^2) (%)	Age dispersion (%)	Fission track age (Ma)	Latitude N	Longitude E
Site 2A (AB 62–AB66)	Pz outcrop Jebel Qumar South	18	0.8599 (17754)	0.304 (77)	2.572 (650)	0.11	0.47	27.4±5.5	N 25°43.748	E 56°05.779
Site 3 (AB67–AB71)	Pz outcrop Jebel Qumar South	16	0.8599 (17754)	0.566 (147)	3.488 (905)	32.81	0.18	23.3±2.6	N 25°43260	E 56°06.400
Site 4 (AB77A–AB77D)	Turonian or younger	16	0.8599 (17754)	0.120 (94)	0.947 (741)	0.03	0.41	28.3±4.7	N 25°60.838	E 56°13.810
Site 5 (AB103)	Turonian or younger Jebel Agah	12	0.8599 (17754)	0.176 (38)	1.647 (354)	44.21	0.01	15.4±2.8	N 25°52.319	E 56°10.311
Site 6 (AB106–AB110)	Tr-outcrop Musandam	5	0.8599 (17754)	0.189 (15)	2.003 (159)	64.9	0.00	13.6±3.8	N 25°47.842	E 56°14.362
Site 8 (AB113–AB114)	Tr-outcrop Musandam	11	0.8599 (17754)	0.229 (48)	2.219 (464)	1.6	0.45	15.4±2.8	N 25°48.562	E 56°12.271

Glass CN-5, Zeta 334.5±22; sample sites 3, 5 and 6 passed the chi-square test at 5% and pooled ages have been calculated; sample sites 2A, 4 and 8 did not pass the chi-square test at 5% and mean ages have been calculated

Table 2 Apatite and zircon fission track analytical data of magmatic samples (see the location of the samples in Fig. 1b)

	Sample	Rock type	Number of grains	ρ_d 10^6 tr/cm^2 (N_d)	ρ_s 10^6 tr/cm^2 (N_s)	ρ_i 10^6 tr/cm^2 (N_i)	P (χ^2) (%)	Age dispersion (%)	Fission track age (Ma)	Latitude N	Longitude E
Apatite	UAE 164[a]	Plagiogranite	13	0.8630 (17818)	0.5072 (82)	1.002 (162)	97.11	0.00	72.6±11.0	2770944	424646
	UAE 169[a]	Pegmatitic gabbro	2	0.8630 (17818)	1.049 (65)	1.969 (122)	90.98	0.00	76.4±12,8	2797594	433909
	UAE 178[a]	Gabbro	20	0.8630 (17818)	0.065 (55)	0.0461 (390)	100	0.00	20.3±3.2	2811441	416203
	UAE 180[a]	Leucocratic part vinagrette	25	0.8630 (17818)	0.8636 (260)	3.062 (922)	100	0.00	40.6±3.9	2781090	423702
Zircon	UAE 180[b]	Leucocratic part vinagrette	7	0.674 (18008)	3.06 (285)	2.36 (220)	52	0.00	46.6±4.3	2781090	423702

[a] Glass CN-5, Zeta 334.5±22; all samples passed the chi-square test at 5% and pooled ages have been calculated; etch pit diameter refers to more Cl-rich than F-rich apatites

[b] CN-1 glass, Zeta 107±2; the sample passed the chi-square test at 5% and pooled age has been calculated

accounting for the refolding of overlying allochthonous nappes (made up of the Hawasina–Sumeini units, as well as the metamorphic sole and overlying Semail Ophiolite).

A single site (UAE 180) remains more problematic, as it yields intermediate, Paleogene (40.6 ± 3.9 Ma) ages. Interestingly enough, zircon from the same sample yielded a pooled FT age of 46.6±4.3 Ma. The apatite and zircon fission track ages fit the ~46–63-Ma fission track ages of the high-pressure eclogites at As Sifah in the southeast near Muscat. One possible interpretation for this would be a partial resetting of apatite and zircon in the vicinity of active hot fluid conduits, as the sample locality is close to a major tear fault dissecting the ophiolite. However, to partially reset the fission track zircon system, relatively high temperatures of >200°C are needed and that seems to be unrealistic to assume. Alternatively, the ages might record a continuous unroofing of the ophiolite occurring between the time of its obduction during the Late Cretaceous and the time of its passive refolding during the Neogene.

Depth migration and construction of the structural section

Iterations between wells calibration, structural interpretation and depth migration have resulted in an accurate depth image of the foreland and central part of the foothills, i.e., in the vicinity of D1, D3 and D4 intersections and westward. In addition to specific values derived from the refraction test and gravity modelling for defining the ophiolite thickness (see Naville et al. 2010), we used more generalized velocity assumptions to generate the depth sections farther to the east, i.e., in the vicinity of D2, where still thick sedimentary units are imaged by seismic reflection.

However, the slight change observed in the altitude of the basement in the inner part of sections D1 and D4 (Figs. 3, 4 and 8) may still result from an inappropriate, still underconstrained velocity model in the east (we could generate a flat or even east-dipping attitude for the basement in the eastern part of line D4 similar to what is proposed for line D1 by increasing the velocity values applied for the depth conversion of Hawasina–Sumeini allochthon). Fortunately, this uncertainty on the current burial depth of the basal decollement will not affect the subsequent kinematic modelling or the overall thermal-burial evolution of the transects, maximum burial and temperature being achieved in both sections long time before to reach the current level of erosion and unroofing.

Cross-section balancing techniques (unfolding) were subsequently applied to the two structural sections in order to check the overall consistency of the interpretations (length and thickness of the various sedimentary units, lateral and vertical offsets along the main faults and so on) but resulting also in realistic restored geometries of the profiles prior to the onset of the deformation (Figs. 4, 6 and 9).

The overall amount of shortening does not exceed 40 km for the platform domain along transects D1 and D4, the actual displacement at the front of Hagab thrust averaging only 15 km. This latter value is close to the amount of late shortening estimated in the Arabian basement, although the Hagab thrust possibly started to develop at an earlier stage of deformation (28 versus 20 Ma FT for the onset of Musandam and Masafi culminations, respectively). It is worth to be mentioned that only part of the deformation was transferred forelandward during the successive increment of deformation (part accounting for the 15 km of shortening measured at the front of Hagab thrust), the additional 25 km of shortening being accounted for by (1) backthrusting at the top of the basement wedge and (2) out-of-sequence thrusting–merging to the surface east of Musandam front, i.e., within the Sumeini–Hawasina allochthon and even locally within the Semail ophiolite.

The solutions proposed here (Figs. 4 and 9) remain relatively conservative as far as the lengths of the former Sumeini slope domain and Hawasina basin are concerned. A major uncertainty still relates to the lithofacies and paleogeographic affinities (either Mesozoic platform or slope facies) of the deep underthrust parautochthonous units that extend between the Musandam outcrops or Biyatah well in the west and the basement backstop in the east, beneath the shallower Sumeini slope and Hawasina basinal allochthon.

Thrustpack forward kinematic modelling

Although both regional transects D1 and D4 have been depth-converted and modelled with Thrustpack, only the work done on D4 will be detailed below. In Thrustpack, pre-existing faults should be defined only for the initial state of the model when they are superimposed on the basement and sedimentary layering (Fig. 9a). The history of deformation, syn-tectonic sedimentation/basin filling and erosion of the emerging units can be then split in as many time steps as considered. Every “unit” (bounded by faults) is treated independently by the software; hence, it could be moved by a user-imposed distance (shortening amount produced during the specified time interval) simulating faulting (both thrusting and normal faulting are possible depending upon the defined sense of transport). After each shortening event, the user can draw one or more units, in foreland and/or hinterland, simulating syn-deformation sedimentation. Again, each of these “syn-tectonic” sedi-

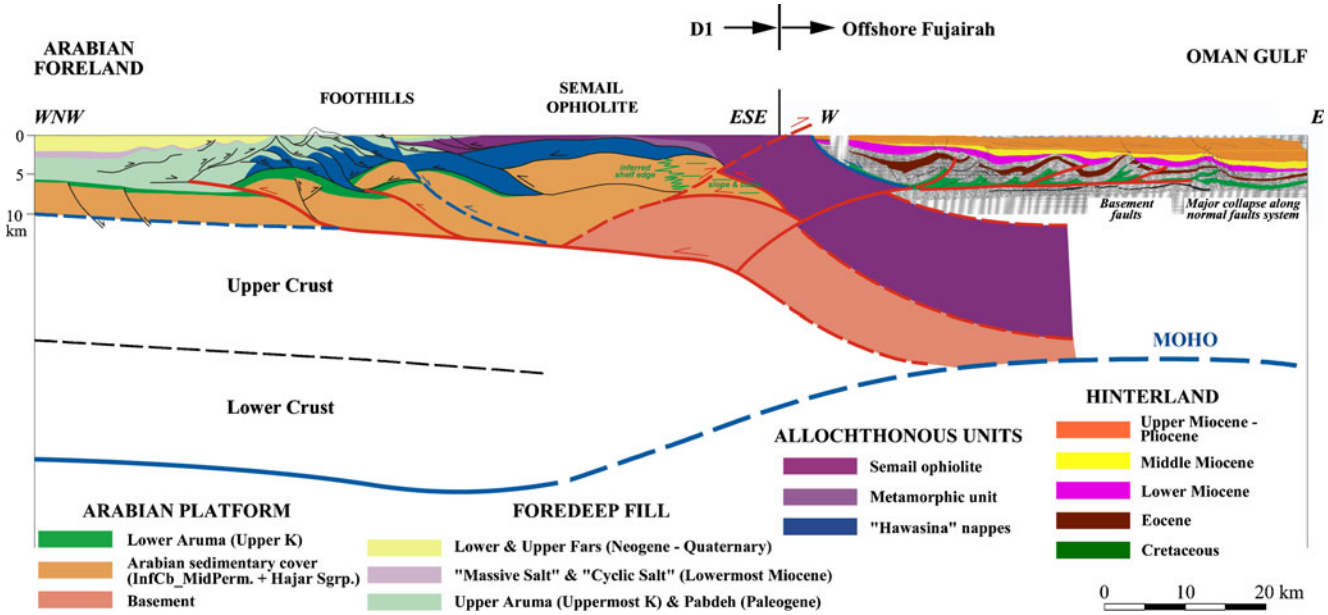

Fig. 8 Crustal architecture of the Oman Range in the UAE along profile D1

mentary units successively added can be moved independently relative to the others during the following deformation steps, so the top and base margins could then represent a flat segment of an active thrust whereas the lateral margin(s) could act as a ramp if drawn inclined. Thrustpack is thus able to accurately simulate both fore- and backthrusts as well as forward-breaking or out-of-sequence shortening. After each shortening event, a user-defined erosional profile can be applied to the model. If considering minor lateral (out of the section plane) transport of sediments, lack of additional source areas and dominantly clastic lithologies, erosion should be applied with care to balance the thickness of the layers deposited in foredeep/hinterland basins. Flexure or uplift is simulated by applying a depth profile at the end of every intermediate model. It should fit the thickness profile of the sedimentary unit(s) and paleobathimetries, depth of the basement or subsidence curves derived from other studies (if existing). In summary, a final model (Fig. 9b) is made up of

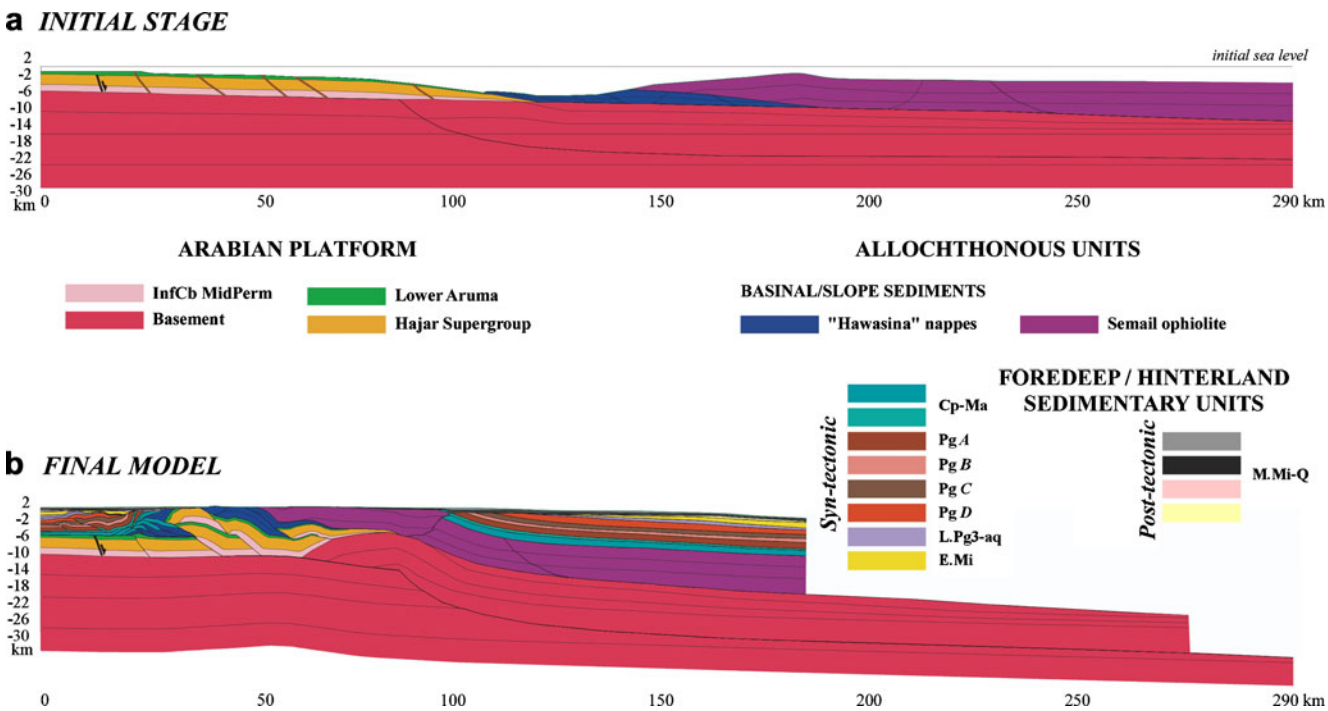

Fig. 9 Initial and final geometry of the Thrustpack section (profile D4)

several intermediate stages characterized by different shortening amounts (or rates, if precise ages can be assigned) that should fit not only the actual structural geometry but also other evidences such as timing of shortening events, thicknesses and gross lithologies of the sediments deposited into the foredeep/hinterland, exhumation magnitudes, timing and position along the belt. Given the complexity of the study area (e.g. Fig. 3), we had to build many intermediate scenarios for each modelled transect before arriving at a good fit because a univocal solution to simulate and quantify the history of deformation is far from straightforward.

The first step of the modelling was to palinspastically restore the profile D4 to its initial, Santonian geometry, just prior to the onset of the underthrusting of the Arabian margin beneath the Sumeini–Hawasina accretionary wedge and Semail Ophiolite (Fig. 9). Because the aim of the forward kinematic modelling was to constrain the burial and thermal evolution of the underthrust Arabian foreland through times (although performed within the project, the latter is not shown herein), we neglected here the period of oceanic subduction and the initial development of the accretionary wedge. For the same reason, the Sumeini slope facies and Hawasina basinal units were collectively treated as a single allochthonous unit although its sediments represent the deep-water counterparts of those covering the Arabian plate. In the model, we also simplified the passive margin series of the Arabian plate, which comprises only three mega-units below the Upper Cretaceous flexural sequence made up of the Aruma Formation.

As discussed previously, the present-day structural geometry is essentially the result of the Neogene convergence and out-of-sequence stacking of the deep Musandam duplex, which ended up by the Middle Miocene. This last episode of deformation accounts for the refolding of the sole thrust of the Sumeini–Hawasina allochthon and is well documented both in the east by Neogene FT ages recorded in the Masafi window and in the west where growth strata are evidenced by seismic imagery in the Fars series.

Seven stages of deformation are discussed below and illustrated in the successive cross-sections along the D4 line (based on the modelling of both D1 and D4, although the former is not shown). Apart from the Upper Cretaceous flexural sequence (Aruma Group) and Neogene growth strata (Fars series), the seismic lines reveal that several unconformities and/or disharmonic features are present within the Pabdeh series, in the proximal deformed foredeep fill. These intra-Pabdeh features can be interpreted as syn-depositional, then implying they could also be linked to the contractional climaxes, thus indicating a long progression of shortening. However, a bio-stratigraphical dating of the Paleogene foredeep sedimentary column at such level of precision is lacking, so the ages labelling several deformation stages in Fig. 6 are somehow arbitrarily chosen, being rather a requirement of the modelling tool. As previously speculated, part of these features (i.e. the summital truncation) could record the Paleogene unbending episode related to a potential slab detachment (although not directly documented), whereas other internal complexities could relate to tectonic imbrications during the development of the frontal Neogene triangle.

The first stage of the forward modelling spans the Campanian to the Early Maastrichtian and comprises the advancement of the Semail ophiolite pushing the Hawasina nappe complex as a whole over the Arabian margin for over 80 km (Fig. 6). The amount of shortening may be larger as we did not consider the expected internal deformation (folding and faulting) at a scale smaller than what can be incorporated into the modelling. We note that during this stage the ophiolite is already exhumed, consistent with the results of the FT measurements on the plagiogranites from the eastern part of the transect. The flexural subsidence post-dating the obduction represents the only tectonic event considered for the Late Maastrichtian and uncertain portion of the Paleogene (Fig. 6).

The continuing convergence led, during the Paleogene, to the formation of the first thrust cutting through the Arabian distal edge in an out-of-sequence manner (referred to as Paleogene stage “a” in Fig. 6). From the rear to the frontal part of the tectonic wedge, this still thin-skinned thrust starts to duplicate the Arabian platform series and the inner Hawasina units in the inner, eastern part of the section, whereas farther west it mainly follows the basal detachment of the former accretionary wedge.

Paleogene stage “b” marks the onset of the thick-skinned tectonics by the abandonment of ophiolite sole and formation of a deep thrust cutting through the Arabian basement. After a relatively long flat at the interface between the basement and sedimentary cover, deep beneath the outcropping ophiolites, this thrust ramps up at different slopes through the Hajar and Hawasina units before inducing the development of a frontal triangle zone in the inner part of the foredeep basin. Note that the structure becomes increasingly complicated in a cross-sectional view.

During the Paleogene stage “c”, shortening proceeds at an almost double amount relative to the previous stage. The same thrust path remains active for most of its length, the noticeable changes occurring in an area near its frontal tip. There the strain is partitioned along many smaller-scale splays merging to the basal detachment of the Hawasina–Sumeini allochthon. A complicated juxtaposition of duplex-type structures and triangle zone develops in the inner part of the foredeep and starts to propagate farther west although at shallower levels. Compared to the previous one, this stage is characterized by a migration of the contractional structures towards the external zones.

Shortening during Paleogene stage “d” amounts to 5 km, being then continuously accommodated by the same thrust in the inner zones but changing to an out-of-sequence breaking through the Hawasina–Sumeini and foredeep fill

in the outer parts. Also, the triangle zone involving the shallower faults seems to migrate towards east.

A reduced convergence of only 2 km is modelled during the Late Oligocene–Earliest Miocene times. The active structures are almost the same as in the previous. Low relief over the exhumed belt would correlate with the creation of a restrictive environment over the foredeep basin where evaporitic precipitation prevails. It is important to note that the top of the Hajar unit in the hanging wall is buried to a depth of almost 4 km.

The last deformation stage took place during the Early Miocene, its main effect being the exhumation of the actual Musandam Peninsula due to the accretion of an underlying blind duplex.

The FT results were of major help in constraining especially the age of exhumation and the amount of overburden removed during Neogene deformation in the case of Musandam Peninsula. In the absence of these new constraints, one may have assumed a different progression of shortening characterized by an earlier onset of its exhumation related to a larger shortening rate, occurring sometime during the Paleogene. Another significant insight is the kinematic linkage assumed between the forward thrusting (duplex formation) and the normal faulting behind along the present-day external boundary of the Dibba zone.

Because of the lack of direct constraints on the seismic profile D4, we did not simulate here the possible effect of an early, pre-obduction episode of foreland inversion. Pre-existing normal faults inherited from the Precambrian to Cretaceous history of the Arabian passive margin and intra-cratonic rift systems have been indeed locally transpressionally reactivated during the Middle Cretaceous (Cenomanian?) in Saudi Arabia and Iraq. Such early deformation might have accounted also for the local unroofing of the Musandam platform prior to the Hawasina–Suneimi nappes emplacement, as attested by unconformable Upper Cretaceous breccias which rest directly in stratigraphic contact on top of Lower Cretaceous, Jurassic, Triassic and even the Permian strata of the Musandam unit and are still preserved beneath the allochthon along the northern border of the Dibba Zone. Other subsurface candidates for early inversion features along transects D1 and D4 can still be found in the underthrust foreland, i.e. in the vicinity of the Margham and Sajaa trends. However, we cannot exclude that part of the former normal faults which localized compressional deformation originated rather from foreland bending during initial periods of thrust loading before becoming also inverted during subsequent Paleogene or Neogene episodes of shortening.

Discussions and conclusion

A good fit has been achieved between the modelled and real cross-section (Fig. 4). Despite the fact that the Santonian stage selected as the initial stage of the model already post-dates the much longer obduction of the Semail ophiolite, our restoration accounts for 120 km of shortening, 80 km being accommodated by the overall length of the Arabian foreland initially underthrust beneath the Hawasina–Sumeini allochthon during the Late Cretaceous, the remaining 40 km being accommodated by tectonic contraction operating within the Arabian foreland itself. In the lower plate, the first 15 km of shortening were accounted for by thin-skinned deformation restricted to the Paleozoic and Mesozoic sedimentary cover, being followed by another 25 km of shortening induced by a thick-skinned duplication of the inner part of the Arabian plate.

Although we favored in the Thrustpack model the hypothesis of a relatively continuous deformation lasting from Late Cretaceous to Neogene, the timing and even the occurrence of individual Paleogene stages of shortening remain speculative. Other kinematic scenarios would instead account for two very distinct episodes of shortening, one in the Late Cretaceous and the other one in the Neogene, with a long period of tectonic quiescence during the Paleogene. Nevertheless, such alternative scenarios must achieve the same amount of shortening, implying only higher deformation rates during shorter periods of active tectonics. The impact on thermal maturity will however change as the residence time of various source rock intervals in higher temperature windows would then increase during the Paleogene.

The FT analyses have provided valuable snapshots on the exhumation times for the different segments of the belt, with erosional unroofing being strongly impacted by the Neogene out-of-sequence duplication of the Arabian platform beneath the Musandam unit and by thick-skinned tectonics which account for a late-stage refolding of the ophiolite and its metamorphic sole in the core of the Masafi anticline. New AFT data from plagiogranites and the occurrence of Late Cretaceous rudists resting directly on top of serpentinized mantle rocks demonstrate that the Semail Ophiolite and underlying Hawasina–Sumeini accretionary wedge were already widely eroded when it reached its present location on top of the Arabian foreland, preventing the lower plate from an ultra-deep burial.

However, because the vibroseis source used for the deep seismic sounding was not sufficient to illuminate the Moho beneath the inner part of the Oman Range, further refraction studies or mantle tomography would still be required to document the fate of the subducted slab. Actually, numerous evidences of Paleogene unbending of the Arabian lower plate, including the erosional summital truncation of the Pabdeh series, can be traced in the inner part of the former Late Cretaceous foredeep, advocating for a possible slab detachment prior to the onset of the Neogene Zagros orogeny. For instance, the relatively small rates of shortening supposed for the Paleogene steps would indicate that an oceanic slab was then detaching. As long as the slab did not fully break, the degree of coupling between the two colliding plates was lower than after the detachment was completed before the Neogene. Renewed

coupling during the Miocene would explain the significant out-of-sequence thrusting that led to the exhumation of Musandam and inversion of some of the former normal faults from the Arabian foreland. Then, as already expressed by Chemenda et al. (1996), the overall plate convergence was transferred to the Makran subduction system, leaving the Oman Range and its foreland devoid of further strain.

Acknowledgements We acknowledge Saleh Al Mahmoudi, Khalid Al Hosani, Abdullah Gahnoog and the Ministry of Energy of the UAE for their long-term support during this project and authorizing this publication. Dr. Q.G. Crowley extracted and provided us the apatite grains from the plagiogranites collected in the field by BGS colleagues. The other apatites and one zircon were separated by Mrs T. Vogel-Eissens at the VU-University. ISES is acknowledged for their support. Two anonymous journal reviewers revised the initial manuscript.

References

Béchennec F, Le Métour J, Rabu D, Villey M, Beurrier M (1988) The Hawasina Basin: a fragment of a starved passive continental margin, thrust over the Arabian Platform during obduction of the Sumail Nappe. Tectonophysics 151:323–343

Béchennec F, Le Métour J, Rabu D, Bourdillon-Jeudy de Grissac C, De Wever P, Beurrier M, Villey M (1990) The Hawasina Nappes: stratigraphy, paleogeography and structural evolution of a fragment of the south-Tethyan passive continental margin. In: Robertson AHF, Searle MP, Ries CA (eds) The geology and tectonics of the Oman region. Geological Society, London, pp 213–224, Special Publication, 49

Béchennec F, Le Métour J, Platel JP; Roger J (1995) Doming and down-warping of the Arabian Platform in Oman in relation to eo-Alpine tectonics. In: Al Husseini MI (ed) GEO'94, the Middle East Petroleum Geosciences, Bahrain, April 1994, I, pp 167–178

Bernoulli D, Weissert H (1987) The upper Hawasina nappes in the central Oman Mountains: stratigraphy, palinspastics and sequence of nappe emplacement. Geodin Acta 1:47–58

Bois C, Damotte B, Roure F (1990) Deep seismic investigations across the Oman range in the UAE. IFP, internal report

Boote DRD, Mou D, Waite RI (1990) Structural evolution of the Suneinah foreland, Central Oman Mountains. In: Robertson AHF, Searle MP, Ries AC (eds) The geology and tectonics of the Oman region. Geological Society, London, pp 397–418, Special Publication, 49

Breton JP, Béchennec F, Le Métour J, Moen-Maurel L, Razin P (2004) Eoalpine (Cretaceous) evolution of the Oman Tethyan continental margin: insights from a structural field study in Jabal Akhdar (Oman Mountains). GeoArabia 9(2):41–58

Callot JP, Breesch L, Guilhaumou N, Roure F, Swennen R, Vilasi N (2010) Paleo-fluids characterization and fluid flow modelling along a regional transect in the Northern Emirates. Arab J Geosci (in press)

Chemenda A, Mattauer M, Bokun AN (1996) Continental subduction and a mechanism for the exhumation of high-pressure metamorphic rocks: new modelling and field data from Oman. Earth Planet Sci Lett 143:173–182

Coffield DQ (1990) Structures associated with nappe emplacement and culmination collapse in the central Oman Mountains. In: Robertson AHF, Searle MP, Ries CA (eds) The geology and tectonics of the Oman region. Geological Society, London, pp 447–458, Special Publication, 49

Coleman RG (1981) Tectonic setting for ophiolite obduction in Oman. J Geophys Res 86:2497–2508

Dunne LA, Manoogian PR, Pierini DF (1990) Structural style and domains of the Northern Oman Mountains (Oman and United Arab Emirates). In: Robertson AHF, Searle MP, Ries AC (eds) The geology and tectonics of the Oman region. Geological Society, London, pp 375–386, Special Publication, 49

Eilrich B, Grotsch J (2003) The Lower Cretaceous carbonate slope-to-platform margin succession near Khatt, United Arab Emirates: sedimentary facies and depositional geometries. GeoArabia 8 (2):275–294

Ellison RA, Woods MA, Pickett EA, Arkley SLB (2006) Geology of the Al Rams 1:50 000 map sheet, 50-1, United Arab Emirates. British Geological Survey, Keyworth, Nottingham, 42 pp

Gass IG, Shelton AW (1986) Thrust tectonics of the eastern Arabian passive continental margin. In: Hydrocarbon potential of intense thrust zones. Abu Dhabi Conference 1986, 1, pp 51–73

Gealey WK (1977) Ophiolite obduction and geologic evolution of the Oman Mountains and adjacent areas. Geol Soc Am Bull 88:1183–1191

Glennie KW (2005) The geology of the Oman Mountains: an outline of their origin. Scientific, Bucks, p 110

Glennie KW, Boeuf MGA, Hughes-Clarke MW, Moody SM, Pilaar WFH, Reinhardt BM (1973) Late Cretaceous nappes in Oman Mountains and their geologic evolution. AAPG Bull 57:5–27

Glennie KW, Boeuf MGA, Hughes Clarke MW, Moody-Stuart M, Pilaar WFH, Reinhardt BM (1974) Geology of the Oman Mountains-Verhandelingen van het Koninklijk. Nederlands Geologisch-Mijnbouwkundig Genootschap 31:423

Goodenough K, Styles MT, Schofield DI, Thomas RJ, Crowley QG, Lilly RM, McKervey J, Stephenson D, Carney J (2010) Architecture of the Oman-UAE Ophiolite: evidence for a multi-phase magmatic history. Arab J Geosci (in press)

Graham GM (1980a) Evolution of a passive margin, and nappe emplacement in the Oman Mountains. In: Panayiotou A (ed) Proceedings, International Ophiolite Symposium, Cyprus, 1979., pp 414–423

Graham GM (1980b) Structure and sedimentology of the Hawasina window, Oman Mountains. PhD thesis, Open University, UK

Gray DR, Kohn BP, Gregory RT, Raza A (2006) Cenozoic exhumation history of Oman margin of Arabia based on low-T thermochronology. Goldschmidt Conference, Abs, doi:10.1016/j.gca.2006.06.428

Hamdan ARA (1990) Maastrichtian Globotruncanids from the western front of the northern Oman Mountains: implications for the age of post-orogenic strata. Journal Faculty of Sciences, United Arab Emirates University, 2., pp 53–66

Hanna SS (1986) The Alpine (late Cretaceous and Tertiary) tectonic evolution of the Oman Ranges: a thrust tectonic approach. In: OAPEC/Symposium on the hydrocarbon potential of intense thrust zones, Abu Dhabi, 2, pp 125–174

Hanna SS (1990) The Alpine deformation of the Central Oman Mountains. In: Robertson AHF, Searle MP, Ries AC (eds) The geology and tectonics of the Oman region. Geological Society, London, pp 341–359, Special Publication, 49

Jahani S, Callot JP, Letouzey J, Frizon de Lamotte D (2009) The eastern termination of the Zagros fold-and-thrust belt, Iran: structures, evolution, and relationships between salt plugs, folding and faulting. Tectonics. doi:10.1029/2008TC002418

Le Métour J, Rabu D, Tegyey M, Béchennec F, Beurrier M, Villey M (1990) Subduction and obduction: two stages in the Eo-Alpine tectonometamorphic evolution of the Oman Mountains. In: Robertson AHF, Searle MP, Ries CA (eds) The geology and tectonics of the Oman region. Geological Society, London, pp 327–341, Special Publication, 49

Lippard SJ, Smewing JD, Rothery DA, Browning P (1982) The geology of the Dibba Zone, northern Oman Mountains; a preliminary study. J Geol Soc Lond 139:59–66

Miller JMcL, Gregory RT, Gray DR, Foster DA (1999) Geological and geochronological constraints on the exhumation of a high-pressure metamorphic terrane, Oman. In: Ring U, Brandon MT, Lister GS, Willet SD (eds) Exhumation processes: normal faulting, ductile flow and erosion. Geological Society, London, pp 241–260, Special Publications, 154

Naville C, Ancel M, Andriessen P, Ricarte P, Roure F (2010) New constraints on the thickness of the Semail ophiolite in the Northern Emirates. Arab J Geosci (in press)

Necea D (2010) High-resolution morpho-tectonic profiling across an orogen: tectonic-controlled geomorphology and multiple dating approach in the SE Carpathians. PhD thesis, Vrije Universiteit University, Amsterdam, ISBN 978-90-8659-432-0, p 147

Nolan SC, Clissold BP, Smewing JD, Skelton PW (1986) Late Campanian to Tertiary paleogeography of the central and northern Oman Mountains symposium on the hydrocarbon potential of intense thrust zones, 2. OAPC, Kuwait, pp 175–200

Nolan SC, Skelton PW, Clissold BP, Smewing JD (1990) Maastrichtian to early Tertiary stratigraphy and palaeogeography of the central and northern Oman Mountains. In: Robertson AHF, Searle MP, Ries CA (eds) The geology and tectonics of the Oman region. Geological Society, London, pp 495–519, Special Publication, 49

Patton TL, O'Connor SJ (1986) Cretaceous flexural history of the northern Oman Mountain foredeep, United Arab Emirates. In: Hydrocarbon potential of intense thrust zones. Abu Dhabi Conference 1986, 1, pp 75–120

Patton TL, O'Connor SJ (1988) Cretaceous flexural history of northern Oman Mountain foredeep. United Arab Emirates. AAPG Bull 72:797–809

Phillips ER, Ellison RA, Farrant AR, Goodenough KM, Arkley SLB, Styles MT (2006) Geology of the Dibba 1:50 000 map sheet, 50-2, United Arab Emirates. British Geological Survey, Keyworth, p 59

Ricateau R, Riché PH (1980) Geology of the Musandam Peninsula (Sultanate of Oman) and its surroundings. J Pet Geol 3(2):139–152

Robertson AHF, Searle MP (1990) The Oman Tethyan continental margin: stratigraphy, structure, concepts and controversies. In: Robertson AHF, Searle MP, Ries AC (eds) The geology and tectonics of the Oman region. Geol Soc Spec Publ 49, pp 3–25

Robertson AHF, Blome CD, Cooper DWJ, Kemp AES, Searle MP (1990) Evolution of the Arabian continental margin in the Dibba Zone, Northern Oman Mountains. In: Robertson AHF, Searle MP, Ries AC (eds) The geology and tectonics of the Oman region. Geol Soc Spec Publ 49, pp 251–284

Roure F, Andriessen P, Breesch L, Broto K, Bruneau J, Chérel L, Collin M, Ellouz N, Faure JL, Guilhaumou N, Jardin A, Muller C, Naville Ch, Ricarte P, Rodriguez S, Swennen R, Tarapoanca M (2006) Deep seismic survey in the Northern Emirates, Part II: main interpretation and modelling report. Ministry of Energy, UAE-IFP Report no. 59 359, p 125

Sassi W, Graham R, Gillcrist R, Adams M, Gomez R (2007) The impact of deformation timing on the prospectivity of the Middle Magdalena sub-thrust, Colombia. In: Ries AC, Butler RWH, Graham RH (eds) Deformation of the Continental Crust: The legacy of Mike Coward. Geol Soc Spec Publ, 272, pp 473–498

Searle MP (1985) Sequence of thrusting and origin of culminations in the northern and central Oman Mountains. J Struct Geol 7:129–143

Searle MP (1988a) Thrust tectonics of the Dibba Zone and the structural evolution of the Arabian continental margin along the Musandam Mountains (Oman and UAE). J Geol Soc Lond 145:53–63

Searle MP (1988b) Structure of the Musandam Culmination (Sultanate-of-Oman and United-Arab-Emirates) and the Straits of Hormuz Syntaxis. J Geol Soc 145:831–845

Searle MP, Cox JS (2002) Subduction zone metamorphism during formation and emplacement of the Semail Ophiolite in the Oman Mountains. Geol Mag 139(3):241–255

Searle MP, James NP, Calon TJ, Smewing JD (1983) Sedimentological and structural evolution of the Arabian continental-margin in the Musandam Mountains and Dibba Zone. United-Arab-Emirates. Geol Soc Am Bull 94(12):1381–1400

Styles MT, Ellison RA, Arkley SLB, Crowley Q, Farrant A, Goodenough KM, McKervey JA, Pharaoh TC, Phillips ER, Schofield D, Thomas RJ (2006) The geology and geophysics of the United Arab Emirates. British Geological Survey, Keyworth

Warburton J, Burnhill TJ, Graham RH, Isaac KP (1990) The evolution of the Oman Mountains foreland basin. In: Robertson AHF, Searle MP, Ries AC (eds) The geology and tectonics of the Oman region. Geological Society, London, pp 419–427, Special Publication, 49

Warrak M (1996) Origin of the Hafit structure: implications for timing the Tertiary deformation in the northern Oman mountains. J Struct Geol 18(6):803–818

Watts KF (1985) Evolution of carbonate slope facies along a Mid Cretaceous segment of the south Tethyan continental margin, the Mesozoic Sumeini Group and the Qumayrah facies of the Muti Formation, Oman. PhD dissertation, Univ. of California, Santa Cruz

Watts KF (1990) Mesozoic carbonate slope faciès marking the Arabian platform margin in Oman: depositional history, morphology and palaeogeography. In: Robertson AHF, Searle MP, Ries CA (eds) The geology and tectonics of the Oman region. Geol Soc Spec Publ, 49, pp 139–160

Watts KF, Blome CD (1990) Evolution of the Arabian carbonate platform margin slope and its response to orogenic closing of a Cretaceous ocean basin, Oman. In: Evolution of carbonate platforms. International Association Sedimentary, Special Publication, 9, pp 291–323

Watts KF, Garrison RE (1986) Sumeini group, Oman-, evolution of a Mesozoic carbonate slope on a South Tethyan continental margin. Sed Geol 48:107–168

Woodcock NH, Robertson AHF (1982) Stratigraphy of the Mesozoic rocks above the Semail Ophiolite, Oman. Geol Mag 119:67–76